Flow," Aeronautical Report LR-343 N.R.C. 6968, 1962, National Research Council of Canada.

[7] Benjamin, B. T., "Theory of the Vortex Breakdown Phenomenon," *Journal of Fluid Mechanics*, Vol. 14, 1962, pp. 593–629.

[8] Bossel, H. H., "Vortex Breakdown Flowfield," *The Physics of Fluids*, Vol. 12, 1969, pp. 498–508.

[9] Gartshore, I. S., "Some Numerical Solutions for the Viscous Core of an Irrotational Vortex," Aeronautical Report LR-378, N.R.C. 7479, 1963, National Research Council of Canada.

[10] Hall, M. G., "The Structure of Concentrated Vortex Cores," *Progress in Aeronautical Sciences*, edited by D. Kücheman, Vol. 7, Pergamon Press, New York, 1966, pp. 53–110.

APRIL 1971 AIAA JOURNAL VOL. 9, NO. 4

Evolution of the Laminar Wake behind a Flat Plate and Its Upstream Influence

L. I. SCHNEIDER*
North American Rockwell Corporation/Space Division, Downey, Calif.

AND

V. E. DENNY†
University of California, Los Angeles, Calif.

Analysis of laminar, two-dimensional, viscous flow of an incompressible fluid over the trailing edge of a vanishingly thin flat plate is presented. A coordinate transformation is introduced which admits sufficient scaling of the problem to enable detailed study of the separating flow and its interactions with the inviscid stream, as well as with a presumed boundary-layer flow in an intermediate region. Second-order boundary-layer theory is applied in an iterative manner to extract a first approximation to the displacement thickness and associated induced pressure distribution. It is found that the near-wake region is nonisobaric, the classical isobaric result of Blasius-Goldstein for displacement thickness being slightly high just prior to the trailing edge and about 10% low downstream. Local corrections to the velocity and pressure distributions are obtained by numerically solving the full Navier-Stokes equations, using the second-order boundary-layer results to establish Dirichlet boundary conditions over a rectangular region enclosing the trailing edge point. It is found that the physical extent of this region is of order $R^{-3/4}$. Within the region, shear at the plate increases with x and becomes very large at the trailing edge. No significant correction to the displacement thickness was found on resolving the second-order boundary-layer problem, using the Navier-Stokes results as inner boundary conditions.

Nomenclature

c_f = drag coefficient, $(2/R)(\partial u/\partial y)|_{y=0}$
c_p = pressure coefficient, $(P - P_\infty)/\rho U_\infty^2$
L = plate length, ft
m = continuity equation, $u_x + v_y$
p = pressure
P = pressure, $lb_m/ft\ sec^2$
r = polar radius
R = Reynolds number, LU_∞/ν
s,t = Cartesian coordinates
u,v = velocity components
U = velocity component, fps
x,y = Cartesian coordinates
α = relaxational parameter
δ^* = displacement thickness
θ = polar angle
λ = integral averaging parameter for difference analogues to equations
ν = kinematic viscosity, ft^2/sec
ρ = density, lb_m/ft^3

Subscripts

e = at the boundary-layer edge
i,j = ijth node point
∞ = at infinity

Received October 16, 1970; revision received September 8, 1970.

* Project Engineer. Member AIAA.

† Assistant Professor, Department of Energy and Kinetics.

1. Introduction

RECENTLY, Plotkin and Flügge-Lotz,[1] using finite difference methods, obtained an improved first approximation to the solution of the trailing edge problem at large Reynolds numbers. Their principal objective was to bridge the gap between the Blasius solution upstream of the trailing edge and the near-wake solution of Goldstein.[2] They solved the Navier-Stokes equations over a region, roughly centered on the trailing edge, whose thickness is several Blasius boundary layers in extent. Dirichlet boundary conditions for the resulting elliptic problem were extracted from the Blasius solution upstream, from the Goldstein solution downstream, and by presuming that the freestream conditions at infinity apply at the region's edge. Thus, they neglect the effect of displacement thickness on the streamwise pressure distribution. Their results indicate existence of a singularity at the trailing edge.

Earlier, several investigators studied the problem using analytical techniques to investigate the full Navier-Stokes equations. The earliest reference appears to be due to Lykoudis,[3] who concluded that the domain of upstream influence of the trailing edge (say Δ) is of the order of a boundary-layer thickness based on the length δ, which in turn is the boundary-layer thickness based on length L measured from the leading edge. Thus, in analogy with ordinary boundary-

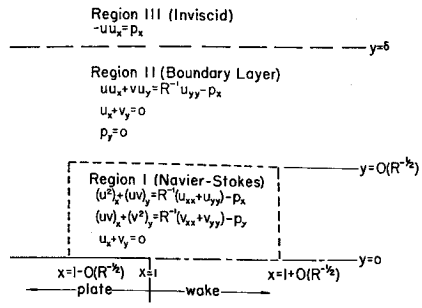

Fig. 1 Schematic diagram of three-layer model for trailing edge problem.

layer theory,

$$\Delta \propto \delta/(R_\delta)^{1/2} = [L/(R_L)^{1/2}]/\{(U_\infty/\nu\ (\mathrm{nu}))[L/(R_L)^{1/2}]\}^{1/2} = R_L{}^{-3/4}L$$

In 1967, Van Dyke[4] also concluded that the full Navier-Stokes equations apply in a circular region of order $R^{-3/4}L$ centered on the trailing edge. He suggests that the method of series truncations be used to solve the problem. In 1966, Dennis and Dunwoody[5] obtained results using series expansions. Results were not obtained in the wake, and the accuracy of the results upstream of the trailing edge have been questioned.[1] In 1964, Imai[6] introduced an Oseen type linearization of the equations in stream function-vorticity form. He, and later Cheng,[7] employed preassigned velocity profiles with undetermined coefficients to linearize the convective terms. The resulting linear problem was then solved by means of integral transform methods. Neither investigator considered the effects of the streamwise pressure distribution as induced by the viscous-inviscid interaction. In fact, a pseudo-boundary condition was generated by assuming constant pressure along the plate. In a subsequent paper, Imai[8] redid the problem using the correct boundary condition of zero velocity at the wall. Both Imai[6,8] and Cheng[7] patched their solution to the first-order boundary-layer solution due to Blasius and Goldstein. It will be shown later that this is not adequate.

Goldburg and Cheng[9] attempted to find a solution to the flow entirely within the framework of boundary-layer theory. They obtained contradictory results and concluded that the solution was perhaps a function of the coordinate system employed. There has been, in fact, considerable controversy as to whether the shear stress and pressure are regular or weakly singular in the vicinity of the trailing edge. The question of the nature of the singularity is of great concern. If the solution technique chosen is not appropriately matched to this singular behavior, the results obtained will be suspect. Such was the case in Ref. 1 where the coordinate grid employed in the numerical solution was much too coarse to accommodate the detailed effects of a singularity which occurs on a scale of $R^{-3/4}L$.

Several investigators have attempted to construct solutions to the Navier-Stokes equations using the results of linearized Stokes flow in an iterative fashion. Carrier and Lin,[10] and later Lugt and Schwiderski,[11] employed this technique. The latter authors assumed that it was possible to develop exact solutions for flows in the vicinity of dihedral angles using linear superposition of the fundamental slow motion integrals. In contrast, Weinbaum[12] claims that the weakly singular solution applies. He reasons that on the Stokes length scale (which is appropriate in regions where pressure-viscous interactions dominate) the velocity would everywhere be continuous, but the pressure would be singular at the trailing edge. The pressure singularity would accommodate rapid changes which are believed to occur on the Knudsen length scale.

Stewartson,[13] using the matched asymptotic expansion (MAX) method, initially solved the problem assuming isobaric flow. More recently,[14] he recognized the importance of the induced pressure distribution (due to displacement thickness) and developed a more complex model (similar to that proposed here) to include this effect. However, his use of linearized airfoil theory (to calculate the inviscid pressure distribution) is inappropriate because the body, though slender, does not exhibit the required small slopes in the immediate vicinity of the trailing edge. Nonetheless, he is able to estimate the upstream influence of the displacement thickness as being $O(R^{-3/8}L)$. The same conclusion was advanced by Messiter.[15] Talke and Berger,[16] employing the method of series truncation,[17] solved the full Navier-Stokes equations in a region surrounding the trailing edge and found the influence of the trailing edge to be $O(R^{-3/4})$. This appears to be the first paper in which the $O(R^{-3/4})$ dependence was found by means of a numerical solution of the trailing edge problem.

The aim here is to obtain a solution to the trailing edge problem which is consistent with second-order boundary-layer theory and, hence, establishes the precise nature of wake evolution and its upstream influence. This will be done by introducing a three-layer model of the problem which applies the full Navier-Stokes equations in an innermost layer adjacent to the plate, the boundary-layer equations in an intermediate layer, and Euler's equation in an outermost layer. A coordinate transformation will be effected whose metric is such as to admit detailed study of the immediate neighborhood of the trailing edge without, at the same time, requiring an excessive number of node points to obtain reasonably accurate difference analogues for the differential equations. Numerical results will be obtained for the pressure distribution induced by displacement thickness, local corrections to the velocity and pressure distributions as predicted by second-order boundary-layer theory, and the drag of the body up to and including the trailing edge.

2. Formulation of the Problem

A three-layer model of the problem is postulated, whose essential features are illustrated in Fig. 1. Note that the full Navier-Stokes equations are introduced in a small sublayer of the flow (Region I) embedded within the boundary layer (Region II) and extending into the wake. It is initially assumed, as part of the numerical procedure, that the effective spatial influence of this region is no more than $O(R^{-1/2})$. Since the plate is aligned with the flow at infinity, only the upper half plane is considered, the flow being symmetrical with respect to the plane of the plate.

Dimensionless forms of the conservation equations for laminar isothermal flow of an incompressible fluid over the plate are

$$(u^2)_x + (uv)_y = R^{-1}(u_{xx} + u_{yy}) - p_x \tag{1}$$

$$(uv)_x + (v^2)_y = R^{-1}(v_{xx} + v_{yy}) - p_y \tag{2}$$

$$-(u^2)_{xx} - 2(uv)_{xy} - (v^2)_{yy} + R^{-1}(m_{xx} + m_{yy}) = p_{xx} + p_{yy} \tag{3}$$

in Region I, where the continuity equation has been eliminated in favor of the pressure equation, retaining in the latter the term $R^{-1}(m_{xx} + m_{yy})$, where $m \equiv u_x + v_y$, in order to increase the convergence rate of the numerical procedure;

$$uu_x + vu_y = R^{-1}u_{yy} - p_x \tag{4}$$

$$u_x + v_y = 0 \tag{5}$$

$$p_y = 0 \tag{6}$$

in Region II; and

$$uu_x = -p_x \tag{7}$$

in Region III. These equations were rendered dimensionless in terms of a reference length L (length of plate), a reference velocity U_∞ (velocity at $y = \infty$), the dynamic pressure in the

freestream ρU_∞^2, and the physical properties of the fluid. Thus, the Reynolds number R equals LU_∞/ν; whereas the dimensional pressure and velocity equal $\rho U_\infty^2 p$ and $U_\infty u$, respectively. The aforementioned equations were reformulated by means of the coordinate transformation

$$s = R^{1/2}[x + 4/(1 + x^{-R^{1/2}})] \quad (8)$$

$$t = 1 - \exp(-R^{1/2}y) \quad (9)$$

The essential property of the $x \rightarrow s$ transformation is depicted in Fig. 2, where it is seen that a small region centered on the trailing edge undergoes significant stretching in the s-t plane.

By means of the chain rule of partial differentiation, it may be established that the original set of equations becomes

$$R^{-1/2}(D_1^2u)_{ss} + R^{-1/2}[(1-t)^2u]_{tt} - [(D_1u + 3R^{-1/2}D_2)u + D_1p]_s - [(1-t)(v - 3R^{-1/2})u]_t + [E_1u - v + R^{-1/2}(1 + E_2)]u + E_1p = 0 \quad (10)$$

$$R^{-1/2}(D_1^2v)_{ss} + R^{-1/2}[(1-t)^2v]_{tt} - [(D_1u + 3R^{-1/2}D_2)v]_s - [(1-t)(v - 3R^{-1/2})v + (1-t)p]_t - [E_1u - v + R^{-1/2}(1 + E_2)]v - p = 0 \quad (11)$$

$$[D_1^2(p - R^{-1}m + u^2)]_{ss} + [(1-t)^2(p - R^{-1}m + v^2)]_{tt} - [3D_2(p - R^{-1}m + u^2) + 2D_1uv]_s + [3(1-t)(p - R^{-1}m + v^2) - 2E_1(1-t)uv]_t + [2D_1(1-t)uv]_{st} + E_2(p - R^{-1}m + u^2) + (p - R^{-1}m + v^2) - 2E_1uv = 0 \quad (12)$$

$$R^{1/2}\{(D_1u)_s - E_1u + [(1-t)v]_t + v\} = m \quad (13)$$

in Region I, where

$$D_1 = R^{-1/2}s_x, \quad D_2 = R^{-1}s_{xx}, \quad E_1 = s_{xx}/s_x, \quad E_2 = s_{xxx}/s_x^2$$

and the equations are written in full divergence form for ease in effecting the finite difference formulation of the problem. In Region II, there obtains

$$D_1uu_s = R^{-1/2}(1-t)^2u_{tt} - (1-t)(R^{-1/2} + v)u_t - D_1p_s \quad (14)$$

$$D_1u_s + (1-t)v_t = 0 \quad (15)$$

$$p_t = 0 \quad (16)$$

while in Region III

$$uu_s = -p_s \quad (17)$$

Boundary conditions for the problem will be discussed along with the discussion of the method of solution.

3. Solution of the Second-Order Boundary-Layer Problem

A first approximation to the solution of the trailing edge problem was obtained by solving the coupled problem as given by Eqs. (14–17) over the half plane $0 \leq t \leq 1$. This was done as follows. First, an implicit difference analogue to the parabolic Eq. (14) was written in Crank-Nicholson form:

$$\bar{u}\bar{D}_1[(u_{i,j} - u_{i,j-1})/\Delta s] = R^{-1/2}\{[(1-t_i)^2/(2\Delta t^2)][(u_{i+1,j} - 2u_{i,j} + u_{i-1,j}) + (u_{i+1,j-1} - 2u_{i,j-1} + u_{i-1,j-1})]\} - [(1-t_i)/(4\Delta t)][R^{-1/2} + \bar{v}][(u_{i+1,j} - u_{i-1,j}) + (u_{i+1,j-1} - u_{i-1,j-1})] - \bar{D}_1p_s|_{i,j} \quad (18)$$

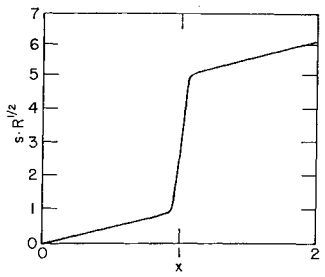

Fig. 2 Properties of longitudinal coordinate transformation.

where

$$\bar{u} = (u_{i,j} + u_{i,j-1})/2, \quad \bar{v} = (v_{i,j} + v_{i,j-1})/2 \quad (19)$$

and

$$\bar{D}_1 = (D_{1,j} + D_{1,j-1})/2$$

The subscripts on u, v, t, D_1, and p_s refer to discrete points on the finite difference grid shown in Fig. 3. Equation (18) assumes the general algebraic form

$$u_{i,j} = A_{i,j}u_{i+1,j} + B_{i,j}u_{i-1,j} + C_{i,j} \quad (20)$$

where the coefficients $A_{i,j}$ through $C_{i,j}$ involve, a priori, unknown values of $u_{i,j}$ and $v_{i,j}$. The $v_{i,j}$ are extracted from a difference analogue to Eq. (15), that is

$$D_1[(u_{i,j} - u_{i,j-1} + u_{i-1,j} - u_{i-1,j-1})/2\Delta s] + (2 - t_i - t_{i-1})(v_{i,j} - v_{i-1,j})/2\Delta t = 0 \quad (21)$$

where

$$v(s,0) = v_{1,j} = 0$$

Boundary conditions for solving the set of simultaneous algebraic Eqs. (20) are at $t = 0$: $u = 0$ for $s < 3R^{-1/2}$, $\partial u/\partial t = 0$ for $s > 3R^{1/2}$; at $t = 1^-$: $u = u_e$. Assuming the Blasius flat plate solution to be valid for $x \leq 0.5$, a first approximation to the solution of the second-order boundary-layer problem was obtained as follows: 1) assume $p_s = 0$ (hence $u_e = 1$), 2) advance the solution to Eq. (20) step by step in the s direction, iterating at a given s station until the coefficients $A_{i,j} \rightarrow C_{i,j}$ are unchanging in the fifth significant figure (and recognizing that coefficients for the first iterate at each station must be calculated using upstream values for $u_{i,j}$ and $v_{i,j}$), 3) extract the displacement thickness δ^*, where

$$\delta^* = R^{-1/2}\int_0^1 [(1-u)/(1-t)]dt$$

at each s station, 4) solve the potential flow problem, where δ^* is the equivalent body, using the Douglas Neumann Program,[18] 5) extract improved values of the u_e [and hence p_s, using Eq. (17)] from 4, and 6) repeat steps 2–5 until δ^* is unchanging in the fifth significant figure.

Considerable manual intervention was required in the solution technique since the first approximation ($dp/dx = 0$) is far removed from the actual solution as one approaches the trailing edge. In this sense, convergence was obtained iteratively only in a figurative sense. In actual practice each iteration is used only as a guide for constructing the succeed-

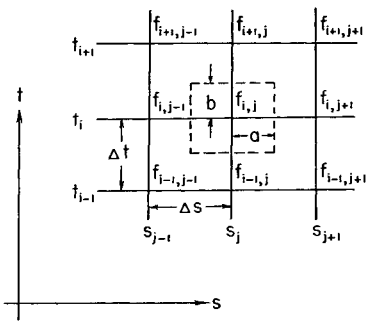

Fig. 3 Node point characteristics for integral averaging technique.

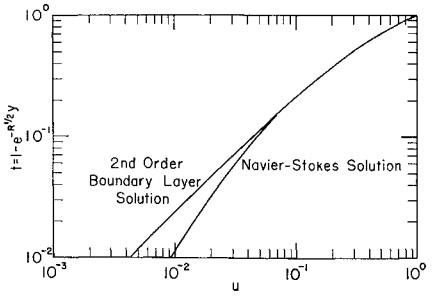

Fig. 4 Confirmation of Navier-Stokes sublayer.

ing iterate. After obtaining a first approximation to the second-order boundary-layer problem, the Region I problem, in which the full Navier-Stokes equations are presumed necessary, was solved.

4. Solution of the Navier-Stokes Problem in Region I

Assuming the full Navier-Stokes equations apply in a subregion of Region II centered on the trailing edge, Eqs. (10–13) were solved numerically, using the second-order boundary-layer results to establish Dirichlet boundary conditions at the edge of Region I. Difference analogues for Eqs. (10–13) were developed in terms of values of the dependent

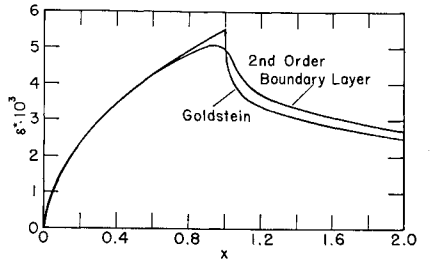

Fig. 5 Effect of second-order boundary-layer theory on δ^*.

variables at the mesh points shown in Fig. 3. Briefly, the procedure entailed fitting a double quadratic in s and t to each of the dependent variables, which was then used to obtain integrally averaged values of the dependent variables and their derivatives over the subregion $4ab$ shown. Thus, for example, if $f = f(s,t)$,

$$\bar{f}_{i,j} = \int_{t_i-b}^{t_i+b}\int_{s_i-a}^{s_i+a} f(s,t)\,ds\,dt/4ab$$

or

$$\bar{f}_{i,j} = \int_{-\lambda}^{\lambda}\int_{-\lambda}^{\lambda} f(\xi,\eta)\,d\xi\,d\eta/4\lambda^2$$

where $\lambda = a/\Delta s = b/\Delta t$. The parameter λ is chosen such that truncation errors in the discretization procedures are minimized. As discussed in Ref. 19, $\lambda = (\frac{1}{2})^{1/2}$ is optimal for linear elliptical problems; and, since $(\frac{1}{2})^{1/2}$ proved to be nearly optimal in this study, it was used throughout. For a double

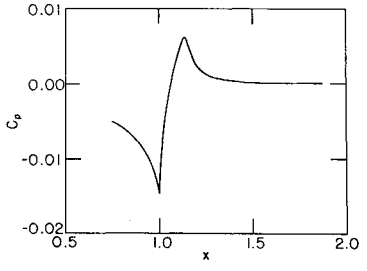

Fig. 6 Induced pressure distribution associated with δ^*.

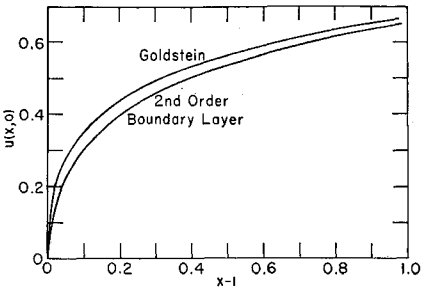

Fig. 7 Evolution of far wake centerline velocity for second-order boundary-layer problem.

quadratic in s and t, $\bar{f}$ thus becomes

$$\bar{f} = (1 - 2\lambda^2/3 + \lambda^4/9)f_{i,j} + (\lambda^2/6 - \lambda^4/18)(f_{i+1,j} + f_{i,j-1} + f_{i-1,j} + f_{i,j+1}) + (\lambda^4/36)(f_{i+1,j+1} + f_{i+1,j-1} + f_{i-1,j-1} + f_{i-1,j+1})$$

Similar algebraic expressions obtain for $\bar{f}_s$, $\bar{f}_t$, etc. On substituting such expressions termwise in Eqs. (10–13), an algebraic approximation to a given equation in the form

$$f_{i,j} = C_{i+1,j}f_{i+1,j} + C_{i-1,j}f_{i-1,j} + R_{i,j+1}f_{i,j+1} + R_{i,j-1}f_{i,j-1} + T_{i+1,j+1}f_{i+1,j+1} + T_{i+1,j-1}f_{i+1,j-1} + T_{i-1,j-1}f_{i-1,j-1} + T_{i-1,j+1}f_{i-1,j+1}$$

obtains. The aforementioned expressions constitute nine-point formulae for each of the dependent variables, and when applied over Region I constitute sets of coupled nonlinear algebraic equations to be solved. This was done by means of the alternating direction implicit-explicit method of Peaceman-Rachford.[20] In so doing, a relaxational coefficient α was introduced to improve the rate of convergence. Thus, for row by row calculations (equations implicit in the s direction), there obtains

$$f_{i,j}^{k+1/2} = \frac{1}{1+\alpha}\left[R_{i,j+1}{}^k f_{i,j+1}{}^{k+1/2} + R_{i,j-1}{}^k f_{i,j-1}{}^{k+1/2} + SR_{i,j}{}^k\right] + \frac{\alpha}{1+\alpha} f_{i,j}{}^k$$

where

$$SR_{i,j} = C_{i+1,j}f_{i+1j} + C_{i-1,j}f_{i-1,j} + T_{i+1,j+1}f_{i+1,j+1} + T_{i+1,j-1}f_{i+1,j-1} + T_{i-1,j-1}f_{i-1,j-1} + T_{i-1,j+1}f_{i-1,j+1}$$

whereas for column by column calculations,

$$f_{i,j}{}^{k+1} = \frac{1}{1+\alpha}\left[C_{i+1,j}{}^{k+1/2} f_{i+1,j}{}^{k+1} + C_{i-1,j}{}^{k+1/2} f_{i-1,j}{}^{k+1} + SC_{i,j}{}^{k+1/2}\right] + \frac{\alpha}{1+\alpha} f_{i,j}{}^{k+1/2}$$

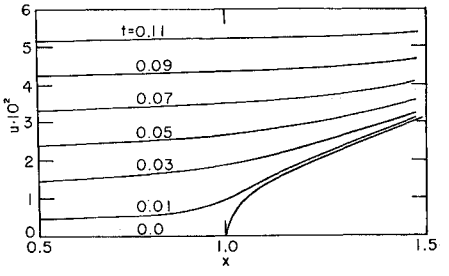

Fig. 8 Longitudinal velocity distribution adjacent to trailing edge.

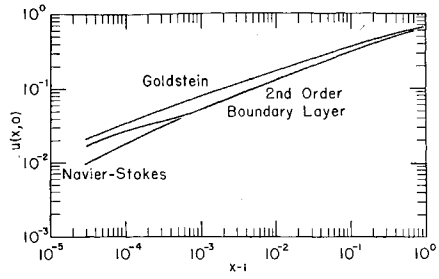

Fig. 9 Evolution of near-wake centerline velocity for Navier-Stokes problem.

where k represents iterate number for a complete cycle of the calculation. Complete details of the algebraic development, as well as optimal values of the iteration parameter α, appear in Ref. 21.

5. Results and Discussion

5.1 Comments on Numerical Procedures

The algebraic equations presented in Sections 3 and 4 were programed in Fortran IV and solved on an IBM 360/65 computer. Approximately six iterations were required to converge the second-order boundary-layer problem, each iterate requiring about seven minutes. Approximately twenty iterations were required to converge the Navier-Stokes problem, where convergence was presumed when the most rapidly varying value for any given dependent variable over the set of node points changed by less than 1%. Running time for each iterate was about five minutes. In all, a single pass through the complete three region problem required nearly 3 hr of computer time. Fortunately, it was not necessary to execute multiple passes because the Navier-Stokes results merged smoothly with the second-order boundary-layer results well within the boundary layer. This is illustrated in Fig. 4, where it is seen that even at the trailing edge station smooth merging occurs for $t \ll 0.5$. However, due to the over-all cost of the numerical calculations, only one value of Reynolds number was investigated ($Re = 10^5$).

5.2 Second-Order Boundary-Layer Solution

As may be seen in Figs. 5–7, the viscous-inviscid interaction is an important feature of the trailing edge problem. As compared with the isobaric result of Blasius-Goldstein,[2] the actual displacement thickness rises less rapidly than, crosses over, and remains about 10% higher than the isobaric result for $x < 1$, $x = 1$, and $x > 1$, respectively. The cusped pressure distribution displayed in Fig. 6 is typical of that associated with air-foils exhibiting rapid changes in curvature such as occurs at joint lines with flaps. The rapid increase in pressure just beyond the trailing edge results in very large longitudinal pressure gradients [$dp/dx = 0(1)$]. As shown in Fig. 7, this adverse pressure gradient tends to retard for considerably greater distances the recovery of the freestream character over that predicted by the Blasius-Goldstein analysis.

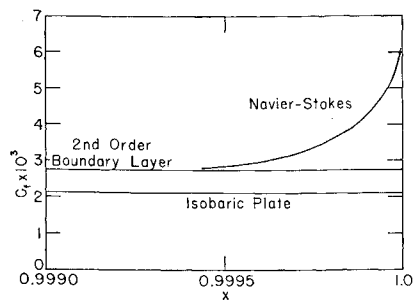

Fig. 10 Effect of longitudinal viscous stresses on the drag of the plate.

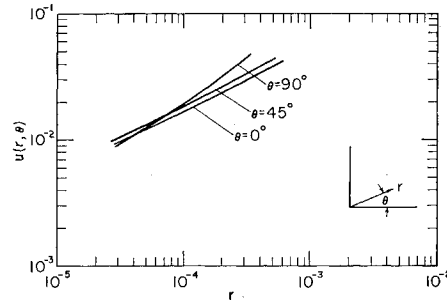

Fig. 11 Flow behavior in immediate vicinity of trailing edge as plotted in polar cylindrical coordinates.

5.3 Navier-Stokes Results

Significant changes in flow behavior over that predicted by second-order boundary-layer theory were found to occur in a small region centered on the trailing edge. The effects are displayed in Figs. 8–10. In Fig. 8, the flowfield, as influenced by separation at the trailing edge, is presented for $t < 0.11$ (for a Reynolds number of 10^5, this corresponds to an overlayer for which $y = 3.7 \times 10^{-4}$, with $R^{-3/4} = 1.78 \times 10^{-4}$). Figure 9 compares the evolution of the near wake center line velocity for the isobaric (Goldstein), nonisobaric (second-order boundary layer) and full Navier-Stokes cases. Again, the Navier-Stokes influence is confined to a region of order $R^{-3/4}$. The rather peculiar character of the second-order boundary-layer result is explained as follows. Near $x = 1+$, the strongly adverse pressure gradient as induced by the δ^* distribution retards the flow. Thus, the center line velocity recovers less rapidly than does the Goldstein result. However, for larger values of x, dp/dx becomes favorable and the velocity recovers more rapidly than, and ultimately merges with, the Goldstein result. In contrast, the Navier-Stokes result, as a consequence of diffusion of momentum upstream by means of viscous stresses, exhibits a relatively lower velocity level and merges with the second-order boundary-layer result from below. The consequences of this momentum deficit are displayed in Fig. 10, where it is seen that the viscous shear on the plate rises as $x \to 1$, becoming very large at $x = 1$. The numerical results are not singular but do indicate that the true behavior is perhaps singular.

For the Reynolds number case studied ($R = 10^{-5}$), $R^{-3/4} = 1.78 \times 10^{-4}$. Inspection of Figs. 4, 9, and 10 reveals the Navier-Stokes solution appears to match the second-order boundary-layer solution on a circle of radius 5×10^{-4} centered on the trailing edge. Thus, the single result obtained here would seem to support the conclusion of other investigators with respect to scaling of $O(R^{-3/4})$.

Since the mesh size employed in obtaining the aforementioned results was approximately 3×10^{-5} (yielding a set of grid points approximately 200×100 in the s and t directions, respectively), the authors believe the effects reported are credible and reflect the essential features of the trailing edge problem. Further confirmation of this conclusion appears in Fig. 11, where the tangential velocity u is plotted in polar coordinates with $x = 1$, $y = 0$ as the origin. To a good approximation, $u \alpha r^n f(\theta)$ with $n \simeq \frac{1}{2}$. Similar results were reported by Weinbaum.[12] No comparison is given with the results of Plotkin[1] since that solution is not applicable to the problem solved here, the grid sizes being much larger than $O(\mathrm{Re}^{-3/4})$.

References

[1] Plotkin, A. and Flügge-Lotz, I., "A Numerical Solution for the Laminar Wake Behind a Finite Flat Plate," *Transactions of*

the ASME, Series E, Journal of Applied Mechanics, Vol. 35, Dec. 1968, pp. 625–630.

[2] Goldstein, S., "Concerning Some Solutions of the Boundary Layer Equations in Hydrodynamics," *Proceedings of the Cambridge Philosophical Society*, Vol. XXVI, 1930, pp. 1–30.

[3] Lykoudis, P., "A Review of Hypersonic Wake Studies," May 1965, RM-4493-ARPA, The Rand Corp., Santa Monica, Calif.

[4] Van Dyke, M., "A Survey of Higher-Order Boundary Layer Theory," SUDAER, No. 326, 1967, Department of Aeronautics and Astronautics, Stanford University, Palo Alto, Calif.

[5] Dennis, S. C. R. and Dunwoody, J., "The Steady Flow of a Viscous Fluid Past a Plate," *Journal of Fluid Mechanics*, Vol. 24, March 1966, pp. 577–595.

[6] Imai, I., "On the Viscous Flow Near the Trailing Edge of a Flat Plate," *Proceedings of the XIth International Congress of Applied Mechanics*, Munich, 1964, pp. 663–671.

[7] Cheng, R. T., *An Investigation of the Laminar Flow Around the Trailing Edge of a Flat Plate*, Ph.D. dissertation, 1967, University of California, Berkeley, Calif.

[8] Imai, I., "A New Approximation for the Viscous Flow Near the Trailing Edge of a Flat Plate," presented at the 12th International Congress of Applied Mechanics, Stanford University, Aug. 26–31, 1968.

[9] Goldburg, A. and Cheng, S. I., "The Anomaly in the Application of PLK and Parabolic Coordinates to the Trailing Edge Boundary Layer," *Journal of Mathematics and Mechanics*, Vol. 10, 1961, p. 529.

[10] Carrier, G. F. and Lin, C. C., "On the Nature of the Boundary Layer Near the Leading Edge of a Flat Plate," *Quarterly of Applied Mathematics*, Vol. III, 1948, pp. 63–68.

[11] Lugt, H. J. and Schwiderski, E. W., "Flow Around Dihedral Angles," *Proceedings of the Royal Society*, Vol. A285, May 1965, p. 382.

[12] Weinbaum, S., "On the Singular Points in the Laminar Two-Dimensional Near Wake Flow Field," *Journal of Fluid Mechanics*, Vol. 33, 1968, pp. 38–63.

[13] Stewartson, K., "On the Flow Near the Trailing Edge of a Flat Plate," *Proceedings of the Royal Society*, Vol. A306, 1968, pp. 275–290.

[14] Stewartson, K., "On the Flow Near the Trailing Edge of a Flat Plate II," *Mathematika*, Vol. 16, Pt. 1, June 1969, pp. 106–121.

[15] Messiter, A. F., "Boundary Layer Flow Near the Trailing Edge of a Flat Plate," *SIAM Journal of Applied Mathematics*, Vol. 18, Jan. 1970, pp. 241–257.

[16] Talke, F. E. and Berger, S. A., "The Flat Plate Trailing Edge Problem," *Journal of Fluid Mechanics*, Vol. 40, Pt. 1, Jan. 1970, pp. 161–190.

[17] Van Dyke, M., "A Method of Series Truncation Applied to Some Problems in Fluid Mechanics," SUDAER No. 247, Department of Aeronautics and Astronautics, Stanford University, 1965.

[18] Giesing, J. P., "Extension of the Douglas Neumann Program to Problems of Lifting Infinite Cascades," LB 31653, July 1964, Douglas Aircraft Company, Los Angeles, Calif.

[19] Schneider, L. I., "Alternating Difference Implicit Techniques for Solution of LaPlace and Poisson Equation on Two Dimensions," TFD 68-129, June 1968, North American Rockwell Corporation, Los Angeles, Calif.

[20] Peaceman, D. W. and Rachford, H. H., "The Numerical Solution of Parabolic and Elliptic Differential Equations," *SIAM Journal*, Vol. 3, 1955, pp. 28–41.

[21] Schneider, L. I., "The Evolution of the Laminar Wake and Its Upstream Influence," Ph.D. dissertation, 1969, University of California, Los Angeles, Calif..

APRIL 1971 AIAA JOURNAL VOL. 9, NO. 4

An Approach to the Dust Devil Vortex

SAMUEL E. LOGAN*
California Institute of Technology, Pasadena, Calif.

A simple analytical model is developed for prescribing the velocity fields in a dust devil, a small intense vortex phenomenon common in arid regions. Since observations by Sinclair indicate that the tangential motion resembles a Rankine combined vortex with superimposed radial inflow near the ground, the model proposed has an "outer" inviscid region of cyclostrophic balance and an "inner" inflow region controlled by viscosity. A perturbation analysis is first performed showing the tangential and radial boundary layer velocity profiles to have the well-known oscillatory nature of the Ekman and Bödewadt solutions. A momentum integral method using these velocity profiles as trial functions is then employed to obtain the functional dependences of the boundary-layer thickness and the integrated radial and vertical mass flows. These are found to depend on the square root of the nondimensional eddy viscosity or inverse Reynolds number of the outer flow, and compare favorably with the measurements of Sinclair.

Nomenclature

a^* = parameter in Burger's vortex solution.
$A(r)$ = amplitude coefficient of radial velocity, perturbation solution
B,D,F,I_1 = velocity profile constants, integral solution
$E(r)$ = amplitude coefficient of radial velocity, integral solution
f,g = radial, tangential trial functions, integral solution
$M(r)$ = integrated inward radial mass flow in boundary layer
p = $p^*/\rho_0^* V_m^{*2}$, dimensionless pressure
p_a^* = ambient pressure
r = r^*/r_m^*, dimensionless radius
r_m^* = dimensional radius of maximum tangential velocity V_m^*
R_0 = $V_m^*/(2\Omega_z^* r_m^*)$, the Rossby number
u_{max} = maximum radial velocity at a given radius
(u,v,w) = $(u^*/V_m^*,\ v^*/V_m^*,\ w^*/V_m^*)$ dimensionless radial, tangential, vertical velocity components
V_m^* = maximum tangential velocity of outer vortex
$W(r)$ = vertical velocity above boundary layer, integral solution
z = z^*/r_m^*, dimensionless vertical coordinate
$\bar{z}$ = stretched vertical coordinate in boundary layer
$\beta(r)$ = $\delta(r)^4 v_0(r)^{8/3}$
$\Gamma_0(r)$ = $v_0 r$, dimensionless circulation of outer flow

Received October 29, 1969; revision received August 12, 1970. This work is based on the paper which won first place in the graduate division at the AIAA National Student Conference, October 1969.[1] The author wishes to thank H. W. Ellsaesser for his suggestion of the problem and initial guidance.

* Graduate Student in Aeronautics, Karman Laboratory of Fluid Mechanics; Fannie and John Hertz Foundation Fellow. Student Member AIAA.